Polarizable Empirical Force Field for Alkanes Based on the Classical Drude Oscillator Model

Igor V. Vorobyov, Victor M. Anisimov, and Alexander D. MacKerell Jr.*

Department of Pharmaceutical Sciences, School of Pharmacy, University of Maryland, Baltimore, Maryland 21201

Received: June 13, 2005; In Final Form: August 1, 2005

Recent extensions of potential energy functions used in empirical force field calculations have involved the inclusion of electronic polarizability. To properly include this extension into a potential energy function it is necessary to systematically and rigorously optimize the associated parameters based on model compounds for which extensive experimental data are available. In the present work, optimization of parameters for alkanes in a polarizable empirical force field based on a classical Drude oscillator is presented. Emphasis is placed on the development of parameters for CH_3, CH_2, and CH moieties that are directly transferable to long chain alkanes, as required for lipids and other biomolecules. It is shown that a variety of quantum mechanical and experimental target data are reproduced by the polarizable model. Notable is the proper treatment of the dielectric constant of pure alkanes by the polarizable force field, a property essential for the accurate treatment of, for example, hydrophobic solvation in lipid bilayers. The present alkane force field will act as the basis for the aliphatic moieties in an extensive empirical force field for biomolecules that includes the explicit treatment of electronic polarizability.

1. Introduction

Aliphatic groups are essential components of all biological macromolecules. Examples include the hydrophobic tails of lipids, the side chains of most amino acids, the backbone and sugar moiety of nucleic acids, and the majority of carbohydrates. Accordingly, when using theoretical models based on empirical force fields it is essential that the aliphatic portion of the force field be treated accurately. Consistent with the importance of aliphatic groups in biomolecules a number of workers have published studies on the treatment of alkanes via empirical force fields based on nonpolarizable or additive models.[1−37] In these studies it has been shown that additive models can accurately reproduce a variety of experimental observables, including selected pure solvent condensed phase properties as well as solvation free energies in aqueous solution. Alkane simulations using nonadditive, polarizable models are still scarce in the literature and have not demonstrated any substantial changes in the molecular properties over the traditional additive force fields.[38−40] Fluctuating charge models were used for the treatment of explicit polarizability in those studies, whereas the classical Drude oscillator model is utilized in this work. Heats of vaporization and molecular volumes were used for the validation of those force fields; however, additional validation of the models using a wider range of condensed phase properties was not performed.

Alkane force fields in the context of biomolecular energy functions have been developed for the CHARMM force field[3−5] as well as other empirical force fields such as GROMOS,[6−9] OPLS,[10,12,41] AMBER,[42−44] and others.[45−63] The majority of alkane force fields have been optimized based on the reproduction of experimental enthalpies of vaporization and vapor pressures and densities, as pioneered by Jorgensen.[41] Recently, free energies of hydration have also been included as target data[3,7l,10,12] and MacKerell and co-workers have developed a protocol for Lennard-Jones (LJ) parameter optimization using a combined ab initio/empirical approach to allow for the relative values of the Lennard-Jones parameters to be better balanced.[3] The alkane LJ parameters determined in that study were then implemented into the CHARMM27 (C27) force field for nucleic acids[64] and lipids.[4] Recently new alkane torsional parameters were developed based on high-level QM calculations and yielded a revised potential referred to as C27r.[4,5]

While the available alkane force fields have been shown to have great utility in studying a wide variety of systems, such additive models have the inherent limitation in that they systematically underestimate the dielectric constant of nonpolar systems. This is due to neglect of electronic polarization such that they cannot account for the dielectric response of the system in the presence of a high-frequency oscillating field giving rise to the optical dielectric constant ϵ_∞.[65] For example, the experimental dielectric constant of propane is 1.796[66] at the normal boiling point (231 K); however, empirical models based on a nonpolarizable energy function typically have dielectric constants of approximately 1 since the electronic polarization is the major contributor to the dielectric response. While this difference seems small, it must be remembered that, according to the Born approximation, the free energy of solvation scales with $(1 - 1/\epsilon)$, where ϵ is the dielectric constant.[67] Accordingly, the difference between a dielectric constant of approximately 1 and 2 will have a significant impact on the free energy of solvation in alkanes. With respect to biological systems, proper treatment of solvation in nonpolar environments is important in the context of lipid bilayers, where compounds that have to cross the bilayer must pass through the aliphatic, hydrophobic central region of the membrane. Thus, proper treatment of the dielectric constant in alkanes represents a critical step in the creation of any force field for biological molecules.

* Address correspondence to this author. Phone: (410)706-7442. Fax: (410)706-5017. E-mail: amackere@rx.umaryland.edu.

10.1021/jp053182y CCC: $30.25
Published on Web 09/08/2005

The present study is a continuation of our ongoing development of a polarizable empirical force field for biological molecules. In the model electronic polarizability is introduced via a classical Drude oscillator,[68−74] which allows for the nonadditivity to be treated via auxiliary particles attached to the atomic centers of the system. Building upon the formulation for treatment of the Drude model in MD simulations via an extended Lagrangian[74] a water model, referred to as SWM4-DP, has been developed and shown to reproduce a variety of experimental condensed phase properties including the dielectric and self-diffusion constants.[75] In this water model the polarizability is treated via the use of a Drude particle on only the oxygen, laying the groundwork for a force field that included polarizability only on non-hydrogen atoms. Studies on ethanol−water systems using the Drude polarizable model demonstrated that the energetic and dynamical properties of neat ethanol and ethanol−water mixtures in ambient conditions are accurately reproduced by this model.[76] Subsequently, a unified protocol for determination of electrostatic parameters (i.e., partial atomic charges and atomic polarizabilities) based on fitting to a series quantum mechanical (QM) perturbed electrostatic potentials (ESP) was developed.[77] In this paper, a novel force field for alkanes based on a polarizable potential energy function in the context of the classical Drude oscillator is presented. It is shown that a variety of experimental and QM target data are accurately reproduced by the force field, including condensed phase properties. In addition, to better put the present force field in the context of previously published alkane force fields, results from the additive C27r force field[4,5] are included.

2. Computational Methods

QM calculations were performed using the Gaussian 98 and Gaussian 03 program suites.[78,79] Geometry optimizations were performed at the MP2(fc)/6-31G(d) level of theory. This level of theory provides molecular geometries consistent with available gas phase experimental data (see the Supporting Information) and it has been previously utilized during optimization of the CHARMM27 all-atom empirical force field parameters for alkanes. QM calculations of the molecular electrostatic potentials were performed on MP2 optimized geometries using the B3LYP hybrid functional[80−82] and the correlation-consistent double-ζ Dunning aug-cc-pVDZ basis set,[83] as previously discussed.[77] Single-point energy B3LYP calculations were performed with the tight convergence criteria producing the target QM ESP maps. QM calculations on the alkane complexes with rare gas atoms were performed at the MP3/6-311++G(3d,3p) level.[3]

Empirical force field calculations were performed with the program CHARMM.[84,85] The simple functional form of the potential energy function from the pairwise additive CHARMM all-atom force field[85] was used with polarizability introduced using the classical Drude oscillator model with some modification described below. In the classical Drude oscillator model the polarizability is introduced by adding massless charged particles attached to polarizable atoms (e.g., only non-hydrogen atoms in the present model) via a harmonic spring with the force constant k_D. The partial atomic charge of a polarizable atom q is redistributed between the Drude particle and atomic core. The sign of the charges on Drude particles q_D has minimal impact due to the point dipole approximation; q_D is chosen to be negative by analogy with the electron charge.[77] The magnitudes of q_D can be unambiguously determined from the atomic polarizabilities using the relationship $\alpha = q_D^2/k_D$. The charge on the atomic core q_c *is* determined by subtracting the Drude charge from the charge on the atom−Drude pair q, such that each atom−Drude pair forms a dipole $q_D \cdot d$, where d is the displacement vector going from the atom to its Drude particle.

Thus, the electrostatic energy term in the additive potential energy function was modified to include interactions between atomic cores and Drude particles, and the term describing the self-energy of a polarizable atom via the harmonic term $1/2k_D \cdot d^2$ was added to the potential energy function.[77] All nonbonded electrostatic interactions involving Drude particles are treated in the same way as electrostatic interactions between real atoms, i.e., via the Coulomb law. For atoms excluded from the nonbonded lists (i.e., 1−2 and 1−3 pairs), the electrostatic term is modified to allow 1−2 and 1−3 screened dipole−dipole interactions, as suggested by Thole.[86] The screening is implemented through the smearing of the charge on the Drude particle and real atom. Then the screened dipole−dipole interactions are calculated via interactions between a smeared charge with a Slater distribution (using the screening parameter 2.6 in all our calculations) and a point charge.[76]

The partial atomic charges and atomic polarizabilities for the Drude polarizable alkane force field were determined from restrained fitting to the B3LYP/aug-cc-pVDZ response electrostatic potential (ESP) maps using MP2/6-31G(d) optimized geometries of alkanes, as per previous protocol.[77] Briefly, the ESP potential grid points were located on concentric nonintersecting Connolly surfaces around the alkane molecule. To determine both atomic polarizabilities and partial atomic charges from the single fitting procedure, a series of perturbed ESP maps was generated, representing the electronic response of the molecule in the presence of a background point charge of magnitude +0.5e placed on Connolly surfaces along alkane chemical bonds and also in the gaps between them to achieve nearly equidistant coverage of the molecular shape. Five alternating Connolly surfaces of perturbation charges and grid points were generated with size factors 2.2 (charges), 3.0 (grid), 4.0 (charges), 5.0 (grid), and 6.0 (charges), where the size factor multiplied by the vdW radius of the corresponding atom determines its distance from the corresponding surface. Fitting was performed using parabolic RESP restraints to the initial values of both the charges and polarizabilities with the weighting factor of 10^{-5} Å^{-2}. Additionally, a flat well potential with the half-width of 0.1e was used for atomic polarizabilities. Fitting to the same charge and polarizability values was imposed for chemically equivalent atoms.

Molecular dynamics (MD) simulations were performed at 1 atm pressure using the new velocity Verlet integrator[74] implemented in CHARMM. The simulations of ethane, propane, butane, and isobutane were performed at 184.55, 231.08, 272.65, and 261.43 K, respectively, which correspond to their normal boiling points. Simulations of long-chain alkanes (heptane and decane) were performed at 298.15 and 312.15 K, at which experimental data for these substances in the liquid phase at 1 atm pressure are available. A Nosé−Hoover thermostat with a relaxation time of 0.1 ps was applied to all real atoms to control the global temperature of the system. A modified Andersen−Hoover barostat with a relaxation time of 0.1 ps was used to maintain the system at constant pressure. Condensed-phase MD simulations were performed using periodic boundary conditions and SHAKE to constrain covalent bonds involving hydrogens.[87] Electrostatic interactions were treated using particle-mesh Ewald (PME) summation[88] with a coupling parameter 0.34 and 6th order spline for mesh interpolation. Nonbond pair lists were maintained out to 14 Å, and a real space cutoff of 12 Å was used for the electrostatic and Lennard-Jones terms with the latter

truncated via an atom-based force switch algorithm,[89] unless noted. Long-range contributions to the van der Waals terms were corrected for as previously described.[90,91]

The extended Lagrangian double-thermostat formalism[74] was used in all polarizable MD simulations where a mass of 0.1 amu was transferred from real atoms to the corresponding Drude particles. The amplitude of their oscillation was controlled with a separate low-temperature thermostat (at $T = 0.1$ K) to ensure that their time course approximates the SCF regimen.[74] A 0.5 fs time step and a force constant of 200 kcal/(mol·Å^2) on the Drude particles was used for the extended Lagrangian polarizable MD simulations of neat alkanes, whereas a 1.0 fs time step and a force constant of 1000 kcal/(mol·Å^2) was used for all other MD simulations. The smaller time step and Drude force constant for the pure solvents was necessary to ensure the adiabatic regimen in extended Lagrangian molecular dynamics (MD) simulations due to the relatively weak electrostatic field in the pure alkanes. In selected cases MD simulations via SCF treatment of the polarizability were performed as a check of results from the extended Langrangian MD methodology. In all cases, similar properties were obtained (not shown) validating the use of the computationally less expensive extended Lagrangian.

A box of 128 molecules was used for the condensed-phase simulations of ethane, propane, butane, and isobutane, whereas 64 molecules were used for the simulation of larger alkanes. It was shown before that this number of molecules is enough to achieve convergence for the additive C27r simulations of heptane.[5] To obtain convergent results, 10 independent MD simulations were run for 150 ps for each box of the neat alkane with different initial velocities, with the final 100 ps used for the analysis. The results of 10 simulations were averaged to get liquid-phase properties and the standard errors were calculated. Alternatively, the simulations were run for 2050 ps with coordinates saved every 0.1 ps for analysis. Properties of interest were calculated over the final 2000 ps of the simulation and compared to those obtained from four 500 ps blocks to check convergence.

Heats of vaporization, ΔH_{vap}, were determined as shown below:

$$\Delta H_{vap} = -\langle U_{liquid}\rangle + \langle U_{gas}\rangle + RT \qquad (1)$$

where $\langle U_{liquid}\rangle$ is the average potential energy of a molecule from the condensed phase simulation, $\langle U_{gas}\rangle$ is the average potential energy of a molecule in the gas phase, R is the gas constant, and T is the temperature. This expression assumes that the sum of kinetic and vibrational energies is equal for the gas and liquid states.[6] Gas-phase simulations required to calculate E_{gas} were performed using Langevin dynamics in the SCF regimen. The same Drude force constant and masses used in the condensed-phase simulations were used along with infinite nonbonded cutoffs. The friction coefficient of 5.0 ps^{-1} was applied to all atoms except for Drude particles. The gas-phase simulations were performed on all the individual monomers extracted from the respective equilibrated alkane box from the condensed-phase MD simulations. These simulations were run for 100 ps for each molecule with the resultant energies averaged over the 64 or 128 monomer simulations. This approach was found to be more efficient than running one long MD simulation especially for long-chain alkanes for which multiple conformers exist.

Isothermal compressibilites, NMR ^{13}C T_1 relaxation times, and self-diffusivities were calculated using the protocol suggested by Klauda et al.[5] The isothermal compressibilities β_T were calculated using average volume fluctuations from ten 150 ps MD simulations using data from the last 100 ps of each simulation. NMR ^{13}C T_1 relaxation times are inversely proportional to corresponding rotational correlation times τ, which are in turn obtained from the integration of reorientation correlation functions of the CH vectors assuming motional narrowing and an effective bond length of 1.117 Å.[5,92] Correlation functions were obtained from long 2050 ps alkane box simulations. Self-diffusion coefficients D_s were calculated based on the same simulations from the slope of the mean-squared displacement vs simulation time[91] using a weighted least-squares fit with weights obtained from averages of eight subgroups of alkane molecules.[5] Calculated values of D_s were corrected for system-size effects as described in Klauda et al.[5]

The static dielectric constants ϵ of the neat alkanes were calculated from the dipole moment fluctuations of the box using

$$\epsilon = \epsilon_\infty + \frac{4\pi}{3\langle V\rangle k_B T}(\langle \mathbf{M}^2\rangle - \langle \mathbf{M}\rangle^2), \qquad (2)$$

where $\mathbf{M}$ is the total dipole moment of the box, $\langle V\rangle$ is the average volume of the box, and ϵ_∞ is the high-frequency or optical dielectric constant ϵ_∞.[75] Time series of $\mathbf{M}$ were obtained from 10 independent simulations of 150 ps using data from the last 100 ps of each simulation and then concatenated into one large time series, which was used for the ϵ calculation from eq 2. The values of ϵ were then averaged over the last 200 ps of this combined time series when they reached a plateau in all simulations. The high-frequency optical dielectric constant ϵ_∞ can be estimated from the Clausius−Mossotti equation, which relates ϵ_∞ to the molecular polarizability.[75,93] However, we used a more direct way of calculating ϵ_∞ from classical fluctuations of induced dipoles as a measure of total polarizability of the box as was proposed by Neumann and Steinhauser[94] and recently used by Lamoureux et al.[75] ϵ_∞ was calculated from the dipole fluctuations of the box associated with the movement of Drude oscillators according to Langevin dynamics at temperature T^* for 10 frozen nuclear configurations extracted from regular molecular dynamics simulations using the equation

$$\epsilon_\infty = 1 + \frac{4\pi}{3\langle V\rangle_{(f)} k_B T^*}(\langle \mathbf{M}^2\rangle_{(f)} - \langle \mathbf{M}\rangle_{(f)}{}^2), \qquad (3)$$

where $\langle ...\rangle_{(f)}$ indicates an average over induced-dipole fluctuations only.[75] It was previously found that the choice of T^* is irrelevant for the calculation of ϵ_∞ since nuclear positions are fixed[75] and thus T^* was chosen to be 0.1 K as for the low-temperature thermostat used in the extended Lagrangian molecular dynamics simulations (see above). For additive CHARMM force field simulations ϵ_∞ was set to 1 since no electronic degrees of freedom are explicitly modeled in this case.

Free energies of aqueous solvation were obtained via free energy perturbations (FEP)[95,96] using the staged protocol developed by Deng and Roux.[97] According to the FEP method, the free energy change ΔG corresponding to the change in the potential energy from U_i to U_j can be calculated as an average over the ensemble of configurations generated with the potential energy U_i:

$$\Delta G = -kT \ln\left\langle \exp\left[-\frac{U_j - U_i}{kT}\right]\right\rangle_{(U_i)} \qquad (4)$$

This technique works only if the perturbation is small enough, otherwise intermediate potential energy surfaces $U(\lambda)$ are constructed where λ is the coupling parameter such that $U(\lambda=0)$

$= U_i$ and $U(\lambda=1) = U_j$.[95,97] The solvation free energy is calculated as a sum of nonpolar and electrostatic contributions:

$$\Delta G_{sol} = \Delta G_{elec} + \Delta G_{np} \quad (5)$$

The electrostatic contribution is calculated using the standard linear coupling scheme with a coupling parameter λ such that the interaction energy $U_{uv}(X,Y)$ between solute u with coordinates X and solvent v with coordinates Y, which is used to calculate ΔG_{sol} using eq 4, can be broken down into:

$$U_{uv}(X,Y,\lambda) = U_{uv}^{np}(X,Y) + \lambda U_{uv}^{elec}(X,Y). \quad (6)$$

The states with $\lambda = 0$ and 1 correspond to the fully discharged and charged solute, respectively. In all FEP simulations λ was changed from 0 to 1 in 0.1 increments.[97] The nonpolar contribution is calculated with all atomic and Drude charges of the solute set to 0. In the protocol the nonpolar contribution is decomposed into dispersive and repulsive contributions using the Weeks, Chandler, and Andersen (WCA) scheme.[98] The slowly varying dispersive term was also calculated using the linear coupling scheme with the coupling parameter ξ:

$$U_{uv}^{np}(X,Y,\xi) = U_{uv}^{rep}(X,Y) + \xi U_{uv}^{dis}(X,Y) \quad (7)$$

ξ was changed from 0 to 1 in increments of 0.1. The repulsive term, due to its r^{12} distance dependence, cannot be easily treated by a linear perturbation but instead is transformed into a soft-core potential. It is calculated in multiple stages with a staging parameter s.[97] The staging parameter s was set to 0.0, 0.2, 0.3, 0.4, 0.5, 0.6, 0.7, 0.8, 0.9, and 1.0. The free energy contributions from simulations run using different staging parameters were summed. The weighted histogram analysis method (WHAM)[99] was used to obtain the free energies from the simulations. The solvation free energies were computed as a sum of the electrostatic, dispersive, and repulsive contributions. Each term was obtained as a difference in the free energy of the solute in water and in a vacuum. Gas-phase simulations were performed using Langevin dynamics as described above. Aqueous phase calculations were performed using the following protocol. First, the alkane molecule was solvated in a box of 250 SWM4-NDP polarizable water[100] molecules and restrained to the center of mass of the box by a harmonic potential with a force constant of 1.0 kcal/(mol·Å^2) acting on all solute atoms. The previously published SWM4-DP water model[75] was modified to follow the convention of the negatively charged Drude particles and its parameters were refitted.[100] The new SWM4-NDP water model has properties nearly identical with those of the SWM4-DP model; parameters defining the SWM4-NDP are summarized in Table S9 of the Supporting Information. The box was then subjected to 500 Steepest Descent (SD) minimization steps followed by a 1000 step Adopted Basis Newton−Raphson (ABNR) minimization. The system was then further equilibrated via a 600 ps NPT simulation at 298.15 K and 1 atm pressure. The FEP simulations were performed using the same conditions, and the samples were collected from the final 40 of two 50 ps trajectories at each value of the scaling/staging parameter. One trajectory is from the simulation running from the scaling parameter 0 to 1, and the other is for the reverse simulation. In all simulations a time step of 1.0 fs, a Drude force constant of 1000 kcal/(mol·Å^2), a Drude mass of 0.4 amu, and a 1.0 K thermostat for Drude particles were used. The remaining simulation parameters were identical with those described above. A similar setup but the TIP3P water model[101] was used for additive CHARMM FEP simulations.

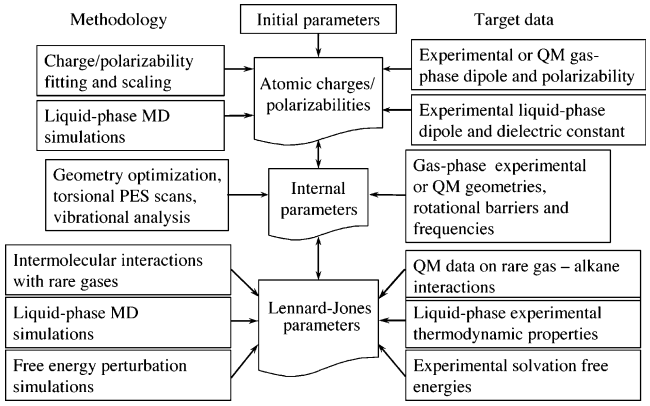

Figure 1. Flow diagram for the alkane parameter optimization for the polarizable CHARMM Drude force field.

3. Results and Discussion

In the present study we have developed empirical force field parameters for alkanes based on a model that explicitly treats electronic polarizability using a classical Drude oscillator, as previously described.[74,75,77,102] In this section results from the Drude polarizable force field calculations for alkanes are presented, along with results from calculations using C27r for comparison. First, the general parametrization strategy is outlined. Then the electrostatic parameter derivation is discussed, following which the internal parameter determination and evaluation is briefly presented. The remaining sections are dedicated to the derivation and validation of Lennard-Jones parameters and final tests of the model in condensed phase simulations of longer alkanes and determination of the free energies of solvation of selected alkanes.

3.1. General Parametrization Strategy. A flow diagram for the alkane parameter development procedure is shown in Figure 1. To a large extent the approach is similar to that used for the CHARMM additive force fields.[3−5] However, the addition of the explicit polarizabilities made necessary the development of a new procedure for the determination of electrostatic parameters. The adopted approach is based on restrained fitting to perturbed QM ESP maps.[77] Experimental or high level QM molecular dipole moments and polarizabilities serve as target data for the electrostatic parameter validation. The dielectric properties of the neat alkanes were also considered as target data allowing for direct examination of the need to scale the atomic polarizabilities as has been shown to be necessary for condensed phase simulations of polar systems.[39,75,77,103−106]

Concerning the internal parameters (i.e., bond, valence angle, Urey−Bradley, dihedral, and improper torsion terms), reproduction of experimental or QM geometries dominate optimization of the equilibrium terms in the energy function while reproduction of vibration spectra and potential energy scans of selected dihedral degrees of freedom are important for optimization of the force constants. All the force constants were initially optimized to reproduce the vibration spectra, following which dihedral parameters that typically involve only non-hydrogen atoms (i.e., the C−C−C−C dihedral parameters in butane) were adjusted to reproduce the conformational energies.

LJ parameters are the most difficult terms to optimize. In the approach developed by Yin and MacKerell,[3] the relative values of the LJ parameters are adjusted based on minimizing the fluctuations of differences between the empirical model and MP3/6-311++G(3d,3p) QM data for interactions between the model compounds and He and Ne atoms. Determination of the absolute values of the parameters is performed via reproduction

TABLE 1: Partial Atomic Charges and Atomic Polarizabilities for the Alkanes[a]

	CH_3			CH_2			CH			
molecule	q(C)	q(H)	α(C)	q(C)	q(H)	α(C)	q(C)	q(H)	α(C)	RMSE
initial guess	−0.270	0.009	2.222	−0.180	0.009	1.835	−0.009	0.009	1.448	
standard fitting protocol										
ethane	−0.243	0.081	2.106							0.91×10^{-3}
propane	−0.202	0.062	2.039	−0.110	0.071	1.680				1.20×10^{-3}
butane *g*	−0.253	0.080	2.169	−0.127	0.070	1.669				1.05×10^{-3}
butane *t*	−0.280	0.068	2.036	−0.124	0.100	1.663				1.16×10^{-3}
isobutane	−0.204	0.060	2.047				0.005	0.067	1.305	1.22×10^{-3}
pentane *gg*	−0.240	0.082	2.075	−0.174	0.085	1.674				0.96×10^{-3}
pentane *gt*	−0.219	0.067	2.043	−0.126	0.069	1.646				1.37×10^{-3}
pentane *tt*	−0.288	0.075	2.021	−0.080	0.061	1.645				1.40×10^{-3}
transferable fitting protocol										
propane	−0.174	0.058	2.040	−0.170	0.085	1.677				1.21×10^{-3}
butane *g*	−0.222	0.074	2.072	−0.164	0.082	1.675				1.10×10^{-3}
butane *t*	−0.126	0.042	2.014	−0.174	0.087	1.653				1.42×10^{-3}
isobutane	−0.180	0.060	2.047				−0.095	0.095	1.302	1.27×10^{-3}
pentane *gg*	−0.249	0.083	2.151	−0.160	0.080	1.667				0.97×10^{-3}
pentane *gt*	−0.180	0.060	2.032	−0.148	0.074	1.652				1.41×10^{-3}
pentane *tt*	−0.114	0.038	2.004	−0.118	0.059	1.635				1.66×10^{-3}
average	**−0.177**	**0.059**	**2.051**	**−0.156**	**0.078**	**1.660**	**−0.095**	**0.095**	**1.302**	

[a] Charges are in electron units and polarizabilities in Å^3. The root-mean-square errors (RMSE) are in potential units (e/Å).

of liquid-phase properties, including heats of vaporization and molecular volumes. This combined approach allows for the relative balance of the different LJ parameters to be determined by QM data, while the use of experimental condensed-phase properties for the absolute values of the parameters overcomes inherent limitations in QM methods with respect to the treatment of dispersion interactions, thereby ensuring that the final parameters yield a model that is representative of the experimental regimen.

Initial guesses for all parameters, except the atomic polarizabilities, are based on the CHARMM additive force fields. Partial atomic charges and LJ and internal parameters except for dihedral energy terms are taken from the work of Yin and MacKerell.[3] The revised C27r torsional potential fitted to high-level QM data from the recent study of Klauda et al is used.[5] Atomic polarizabilities are based on Miller's ahp values[107] adopted for use with the heavy atom polarizability scheme used presently.[77] The results associated with the final parameters along with results from the additive C27r force field will be presented except where noted.

3.2. Electrostatic Parameter Determination. The electrostatic parameter determination is the first step in the Drude polarizable force field development for alkanes. In the additive CHARMM force field the partial atomic charge of 0.09 was assigned to aliphatic hydrogens and CH_x carbon charges were selected to yield a neutral total charge on the corresponding CH_3, CH_2, or CH group.[3,108] The value of 0.09 was assigned to q(H) empirically to refine the butane gauche−trans energy difference.[1] Partial atomic charges and atomic polarizabilities for the Drude polarizable alkane force field were determined from restrained fitting to perturbed QM ESP maps.[77] The obtained partial atomic charges and atomic polarizabilities are given in Table 1. For most compounds the fitted electrostatic parameters are close to the initial values. However, there is one substantial difference. As mentioned above, all CH_x groups are assumed to be electroneutral in the additive CHARMM force field. The fitted values of partial atomic charges for the alkanes, excluding ethane, do not maintain this electroneutrality. In most cases negative charge accumulates on the terminal CH_3 groups, with the central CH_2 and CH groups acquiring a net positive charge. The largest charge flow occurs for the trans conformer of butane: 0.076 e from each CH_2 group is transferred to the adjacent CH_3 group. While such a scenario may be considered formally correct, the lack of electronic neutralitiy on the CH_x group impedes the transferability of short-chain alkane parameters to longer hydrocarbons. While one would expect to obtain electrostatic parameters for the long-chain alkanes via the ESP fitting protocol, such an approach is not tractable due to their flexibility such that all stable conformations should be taken into account during fitting. To overcome this problem, electrostatic parameters for long-chain alkanes will be obtained via the use of transferable values for the CH_3, CH_2, and CH groups. Toward this end a transferable fitting protocol was developed in which charge electroneutrality of CH_x groups was artificially imposed such that $q(\mathrm{C}) = -xq(\mathrm{H})$, where x is the number of hydrogens covalently linked to the carbon. The fitted values of charges and polarizabilities after the transferable fitting are included in Table 1. Root-mean-square (RMSE) values for both regular and transferable fitting are comparable, indicating that the quality of the fitting is not degraded significantly due to the presence of the additional restraint. The atomic polarizabilities also did not significantly change with respect to the standard fitting results. However, the partial atomic charges underwent substantial changes. In most cases, both C and H charges of the terminal CH_3 groups decreased in magnitude, with the remaining charge transferred to the other CH_x groups. The final transferable electrostatic parameters were obtained by averaging over propane, isobutane, butane trans and gauche, and pentane *tt*, *tg*, and *gg* conformers for CH_3 and CH_2, excluding isobutane for the latter, while the values for CH were based on fitting to isobutane. This averaged set of charges and polarizabilities at the bottom of Table 1 were used in all other calculations of the polarizable alkanes.

Validation of the atomic charges/polarizabilities was performed by calculating molecular dipoles and polarizabilities for comparison with QM and/or experimental values (Table 2). The alkane dipole moments are very small, all being less than 0.2 D. B3LYP calculations reproduce the absolute magnitude of propane and isobutane dipole moments reasonably well. The Drude model also satisfactorily reproduces the magnitude of the B3LYP propane dipole moment. For other alkanes the quality of the agreement is poorer for both the Drude polarizable and CHARMM27 models. Scaling of the partial atomic charges was suggested in our previous work[77] to obtain good agreement

TABLE 2: Molecular Dipole Moments and Polarizabilities

				Drude	
	exp[a]	B3LYP	C27r	not scaled	scaled[b]
molecular dipole moments (D)					
ethane		0.000	0.000	0.000	0.000
propane	0.084	0.096	0.002	0.093	0.108
butane *g*		0.104	0.044	0.153	0.175
butane *t*		0.000	0.000	0.000	0.000
isobutane	0.132	0.147	0.012	0.237	0.226
pentane *gg*		0.069	0.047	0.178	0.176
pentane *gt*		0.074	0.033	0.143	0.132
pentane *tt*		0.097	0.019	0.080	0.104
molecular polarizabilities (Å^3)					
ethane	4.47	4.31	0.11	4.06	2.99
propane	6.29	6.14	0.17	5.86	4.28
butane *g*		7.91	0.22	7.65	5.55
butane *t*	8.20	7.99	0.22	8.01	5.75
isobutane	8.14	7.98	0.21	7.58	5.54
pentane *gg*		9.65	0.27	9.46	6.82
pentane *gt*		9.77	0.27	9.91	7.05
pentane *tt*	9.99	9.85	0.27	10.28	7.24

[a] Experimental values are from ref 66. [b] The atomic polarizabilities were scaled by a factor of 0.724 as in refs 75 and 77.

with the reference values. However, such scaling is not applicable for alkanes since the magnitudes of the dipole moments are so small that even small differences of 0.1 D would result in unreasonable scaling factors.

The experimental and/or B3LYP molecular polarizabilities are generally well reproduced by the Drude model with the differences all being less than 6% (Table 2). For instance, the empirical molecular polarizability of ethane is underestimated by 5.8% whereas that of the *tt* conformer of pentane is overestimated by about 4.5%. The additive CHARMM force field lacks explicit electronic polarization although the contribution of the molecular distortion to the polarizability response is still present and was calculated (Table 2). Thus, the use of transferable electrostatic parameters for the alkanes yields satisfactory agreement with the molecular dipole moments and polarizabilities.

3.3. Internal Parameter Determination. Internal parameters were optimized to reproduce target data on the geometries, vibrational spectra, and conformational energies of the model alkanes. Target data for the geometries included MP2/6-31G* geometries along with survey data of the Cambridge Structural Database (CSD), with the results shown in Table S1 of the Supporting Information. In all cases direct transfer of the additive internal parameters was appropriate, as only minor changes in the bond and angles between C27r and the Drude model occur. This is also true for the bond and angle force constants as evidenced by the vibrational spectra of ethane, propane, butane, and isobutane being nearly identical and in good agreement with the target MP2/6-31G(d) spectra (Tables S2 to S5 of the Supporting Information, respectively). The only significant difference occurred in the CCCC torsion term for butane. This term will be affected by 1,4 and beyond intramolecular nonbonded interactions, which differ between the two models and indicates that the dihedral parameters influencing the conformational energies of the alkanes cannot be directly transferred from the additive to the polarizable model.

Fitting of dihedral parameters involving only carbons (i.e., the various C−C−C−C parameters) was performed targeting hybrid QM potential energies of approximately CCSD(T)/cc-pVQZ quality.[4,5] Significant modifications of the parameters were required (Table S6 of the Supporting Information), yielding good agreement with the QM target data. The quality of the agreement was present for both the relative energies of the minima (Table 3) and the energy barriers (Table S7 of the Supporting Information). Analysis of the energy surfaces for the compounds studied showed the Drude model, as well as C27r, to yield good overall agreement with the QM data (Figures S1 to S7 of the Supporting Information). Quantitative assessment of the quality of fit based on average absolute and root-mean-square (RMS) errors validates this conclusion (Table 4). Thus, direct transfer of the C27r internal parameters, with the exception of the dihedral parameters associated with the C−C−C−C torsions, yields satisfactory agreement with the target data. The ability to directly transfer many of the internal parameters is suggested to be due to the relatively small impact of the electrostatic terms on the related geometries and frequencies; it is anticipated that with polar compounds such direct transfer will not be appropriate due a larger impact of electrostatics on geometries and vibrations as well as conformational energies.

TABLE 3: Relative Conformational Energies[a] for the Minima of Selected Alkanes

	QM	Drude	Δ*E*	C27r	Δ*E*
butane					
t	0.00	0.00	0.00	0.00	0.00
g	0.63	0.61	−0.02	0.59	−0.04
pentane					
tt	0.00	0.00	0.00	0.00	0.00
tg	0.62	0.65	0.03	0.59	−0.03
gg	0.99	1.16	0.17	1.12	0.13
g′g	2.85	2.79	−0.05	2.82	−0.03
hexane					
ttt	0.00	0.00	0.00	0.00	0.00
tgt	0.60	0.61	0.01	0.56	−0.04
tgg	0.93	1.01	0.08	1.02	0.09
gtg	1.18	1.20	0.02	1.08	−0.10
g′tg	1.32	1.21	−0.11	1.23	−0.09
tgg	2.74	2.70	−0.04	2.67	−0.07
heptane					
tttt	0.00	0.00	0.00	0.00	0.00
tgtt	0.56	0.53	−0.03	0.53	−0.03
tggt	0.87	0.86	−0.01	0.93	0.06
tgtg	1.14	1.10	−0.04	1.04	−0.10
tgtg′	1.30	1.15	−0.15	1.20	−0.10
tgg′t	2.54	2.48	−0.06	2.60	0.06

[a] Energies are in kcal/mol with respect to global minima.

TABLE 4: Average Absolute (AAE) and Root Mean Square (RMSE) Errors[a] of Empirical with Respect to QM Torsional Potential Energy Surfaces for Rotation around C−C Bonds

		C27r		Drude	
molecule	no.	AAE	RMSE	AAE	RMSE
butane	15	0.056	0.219	0.022	0.145
pentane	30	0.014	0.171	0.042	0.183
hexane	35	0.001	0.143	0.046	0.154
heptane	38	0.010	0.139	0.011	0.140
all	**118**	**0.004**	**0.160**	**0.029**	**0.157**

[a] Errors are in kcal/mol.

3.4. Lennard-Jones Parameter Optimization. LJ parameters were optimized employing the combined ab initio/empirical approach,[3] as described above. Initial parameter optimization was performed using the model compounds ethane, propane, and isobutane. Ethane was used to optimize the LJ parameters for the methyl (CH_3) groups. These were then transferred to propane and isobutane, which were used to optimize the methylene (CH_2) and methine (CH) parameters, respectively. The resultant parameters were then applied to the longer alkanes to verify their transferability. In addition, calculations of the free energies of aqueous solvation afforded an additional test of the resulting model.

TABLE 5: RMS Fluctuations for the Differences and Ratios between the QM and CHARMM Minimum Interaction Energies and Distances for the Alkane−Rare Gas Interactions[a]

	R_{min} (Å)		E_{min} (mkH)	
complex	C27r	Drude	C27r	Drude
		difference		
ethane/He	0.098	0.098	22.9	23.0
ethane/Ne	0.052	0.052	77.9	78.1
propane/He	0.099	0.101	40.3	41.5
propane/Ne	0.064	0.065	60.6	65.1
isobutane/He	0.109	0.115	40.4	40.5
isobutane/Ne	0.072	0.077	48.1	49.0
		ratio		
ethane/He	0.028	0.028	0.201	0.188
ethane/Ne	0.016	0.016	0.069	0.069
propane/He	0.023	0.024	0.225	0.241
propane/Ne	0.018	0.018	0.079	0.083
isobutane/He	0.027	0.027	0.199	0.165
isobutane/Ne	0.020	0.021	0.083	0.078

[a] RMS fluctuations of the differences and ratios as calulated in Yin and MacKerell.[3]

Presented in Table 5 are the RMS fluctuations of the differences and ratios between the QM and empirical model for the interactions with the rare gases (see Table S8 of the Supporting Information for results for the individual interactions) and in Table 6 the results from the pure solvent calculations are presented. The RMS fluctuation data are used to optimize the relative balance of the LJ parameters rather than the RMS or average difference between a set of interactions (e.g., ethane with He) as the differences can be finite but the fluctuations about the average difference should approach zero indicating that all interactions are offset by a similar amount. The need for such an offset is based on the limitations in QM methods in treating dispersion interactions.[3,109−111] Comparison of the results for the polarizable model shows them to be similar to the C27r model, although the latter model is typically slightly better. Such similarity is expected as the same optimization approach was used for both force fields, with the final parameters for the two models being similar (Table 7). The only exception occurs with atom type CT1 associated with isobutane, where the central CH moiety was not explicitly parametrized for C27r via the combined approach.

While improvements with respect to the QM data were not achieved with the polarizable model relative to C27r, significant improvements in the pure solvent properties were obtained. Heats of vaporization and molecular volumes for a variety of alkanes are shown in Table 6 for both the additive and polarizable models. In all cases, except ΔH_{vap} for ethane, the Drude model reproduces the experimental target data within 2%. Notably, upon going from the short alkanes, for which the parameters were explicitly optimized, to the longer alkanes, the Drude model still yields quite good agreement with experiment. With C27r, the molecular volumes for the longer alkanes are in good accord with experiment, but the ΔH_{vap} values are again systematically underestimated, with the differences approaching 18%. Thus, robust optimization of the LJ parameters in the polarizable model yields a force field that satisfactorily treats the energies and densities of neat liquids of both short- and long-chain alkanes as well as the branched isobutane. These results represent an improvement over the C27r model, especially with respect to the longer chain alkanes. However, ongoing work in our laboratory indicates that the limitations in C27r are related to the parameters rather than the polarizable model being able to more accurately treat both the short- and long-chain alkanes (Vorobyov and MacKerell, work in progress).

In addition to the heats of vaporization and densities the isothermal compressibility of heptane and decane was checked. The results, shown in Table 8, show the polarizable model to be in better agreement with experiment as compared to C27r. This agreement is quite good for decane, though the calculated value for heptane is still somewhat overestimated as compared to experiment. The quality of the agreement again indicates the validity of the application of the force field optimized against short chain alkanes for longer chain species.

Additional pure solvent simulations were undertaken to test for possible size effects in obtained condensed phase results. These were performed on neat propane at 231.08 K and heptane at 312.15 K using 256 and 128 molecules, respectively, using ten 150 ps simulations for each system, as used for the results in Table 6. Both the heats of vaporization (4.47 ± 0.01 and 8.44 ± 0.04 kcal/mol for propane and heptane, respectively) and molecular volumes (124.8 ± 0.3 and 249.2 ± 0.4 Å^3 for propane and heptane, respectively) are in good agreement with data in Table 6 obtained using the smaller boxes. These results indicate that the size of the simulation boxes used in the present study are not biasing the calculated results.

Dynamic properties of the empirical models are important as they will impact properties such as viscosity of hydrocarbons, including those in bilayer interiors. Accordingly, self-diffusion coefficients, D_s, and T_1 relaxation times were calculated for the polarizable model and are compared with experiment and results from simulations using C27r. The D_s values for the polarizable model, included in Table 8, underestimate experiment by 4% to 11%, while C27r values overestimate the experimental data by 5% to 9%. In contrast, the T_1 relaxation times (Figure 2) show the polarizable model to be in better agreement with experiment. To allow for a qualitative estimation of convergence T_1, results for both the chain ends are presented individually along with results from two simulations with the Drude model shown for decane. For both C27r and the polarizable model the results are satisfactorily converged. Comparison of the absolute values of the experimental, C27r, and Drude T_1 values shows the polarizable force field to be in much better agreement with experiment, though the heptane results are still overestimated. The significant overestimation of the T_1 values by C27r for both heptane and decane is consistent with previous results, although the self-diffusion constant for heptane was only slightly overestimated in that study.[5] In addition, the polarizable force field satisfactorily reproduces trends in T_1 values as a function of chain position, with a low value for the terminal carbons, an increase upon going to carbon 2, and a gradual decrease moving toward the middle of the molecules. Minor inconsistencies in this trend for the Drude polarizable simulations of decane may be attributed to the convergence issues. Thus, the present results show the polarizable force field to be in better agreement with the T_1 data than C27r while the self-diffusion constants are underestimated in contrast to C27r, which are systematically overestimated.

Changes in T_1 values and self-diffusion constants upon going from C27r to the polarizable model are consistent. The smaller T_1 values indicated slow relaxation of the C−H vectors consistent with the lower self-diffusion values. It should be noted that both models have similar intrinsic conformational energies (Tables 3 and 4 and Table S7 of the Supporting Information) due to the same QM target data being used to optimize the dihedral parameters. Analysis of dihedral probability distributions from the heptane MD simulations confirmed this similarity

TABLE 6: Comparison of Empirical and Experimental Liquid-Phase Properties of Neat Alkanes[a]

		experimental data		C27r		Drude	
	T (K)	V_m	ΔH_{vap}	V_m	ΔH_{vap}	V_m	ΔH_{vap}
ethane	184.55	91.8[b,f]	3.53[b,f]	91.8 ± 0.3	3.42 ± 0.01	91.6 ± 0.3	3.42 ± 0.01
propane	231.10	125.7[b,f]	4.51[b,f]	126.0 ± 0.2	4.28 ± 0.01	124.5 ± 0.4	4.48 ± 0.01
butane	272.65	160.5[b,f]	5.37[b,f]	164.1 ± 0.4	5.05 ± 0.04	160.9 ± 0.3	5.41 ± 0.03
isobutane	261.43	162.5[b,f]	5.12[b,f]	162.3 ± 0.5	4.82 ± 0.02	160.6 ± 0.3	5.03 ± 0.02
heptane	298.15	244.9[b,f]	8.76[e]	248.2 ± 0.3	7.24 ± 0.05	243.9 ± 0.3	8.74 ± 0.05
	312.15	249.1[d]	8.53[e,g]	254.3 ± 0.5	6.97 ± 0.05	249.2 ± 0.5	8.48 ± 0.06
decane	298.15	325.2[c]	12.28[e]	327.7 ± 0.6	10.29 ± 0.07	323.0 ± 0.3	12.42 ± 0.06
	312.15	330.0[d]	12.01[e,g]	336.0 ± 0.5	9.86 ± 0.07	328.4 ± 0.3	12.09 ± 0.07

[a] Molecular volumes V_m are in Å^3, heats of vaporization are in kcal/mol. [b] Experimental data from ref 114. [c] Experimental data from ref 66. [d] Experimental data from ref 5. [e] Experimental data from ref 115. [f] Data were calculated using the linear interpolation between two closest data points. [g] Data were calculated using the empirical equation given in the reference.

TABLE 7: Optimized LJ Parameters of Aliphatic Carbon and Hydrogen Atoms from the CHARMM27 and Drude Polarizable Force Field[a]

	C27r		Drude	
type	$R_{min}/2$	ϵ	$R_{min}/2$	ϵ
CT1	2.275	0.020	2.000	0.032
CT2	2.010	0.056	2.010	0.056
CT3	2.040	0.078	2.040	0.078
HA1	1.320	0.022	1.340	0.045
HA2	1.340	0.028	1.340	0.035
HA3	1.340	0.024	1.340	0.024

[a] R_{min} in Å and ϵ in kcal/mol.

TABLE 8: Comparison of Experimental and Calculated Self-Diffusion Coefficients and Isothermal Compressibilities of Neat Liquid Alkanes[a]

	heptane		decane	
	298.15 K	312.15 K	298.15 K	312.15 K
isothermal compressibilities, β_T				
exptl		14.13		10.80
C27r		20.51 ± 5.33		14.32 ± 1.36
Drude		17.16 ± 2.13		10.34 ± 0.95
self-diffusion constants, D_s[b]				
exptl[c]	3.13	3.73	1.38	1.74
C27r	3.33 ± 0.01	3.95 ± 0.01	1.46 ± 0.00	1.89 ± 0.01
Drude	2.80 ± 0.01	3.52 ± 0.01	1.32 ± 0.00	1.59 ± 0.01

[a] Self-diffusion constants in units of 10^{-5} cm^2/s and isothermal compressibilities in 10^{-10} m^2/N. Calculated isothermal compressibility values represent the average of results from ten 150 ps MD simulations averaged over the final 100 ps of each simulation with the errors being the corresponding standard deviations. Self-diffusion constants were obtained from 2 ns production simulations on systems with 64 molecules, with those systems divided into eight 8 molecule blocks for which average values were obtained with the reported values being the averages and standard errors over those 8 blocks. [b] Calculated self-diffusion coefficients were corrected for system-size effects as previously reported.[5] [c] Experimental results are from ref 116.

(not shown). Thus, the differences in T_1 and D_s values may be assumed not to be due to intrinsic flexibility of the models, but to interactions of the molecules with their environment. This conclusion is consistent with the heats of vaporization results (Table 6), showing larger values for the Drude model versus C27r. Overall, this presents a scenario where the enhanced interactions required to obtain accurate heats of vaporization in the polarizable model lead to a decrease in mobility. In the present situation this leads to the polarizable model underestimating the D_s values while, in the case of decane, yielding T_1 values in good agreement with experiment. The inability to properly treat both the T_1 and D_s values in heptane with C27r was previously suggested to be due to "small errors in the detailed shape of the molecular surface".[5] The present results for the polarizable model are consistent with this conclusion, indicating an inherent limitation in the use of spherical atoms in the potential energy function.

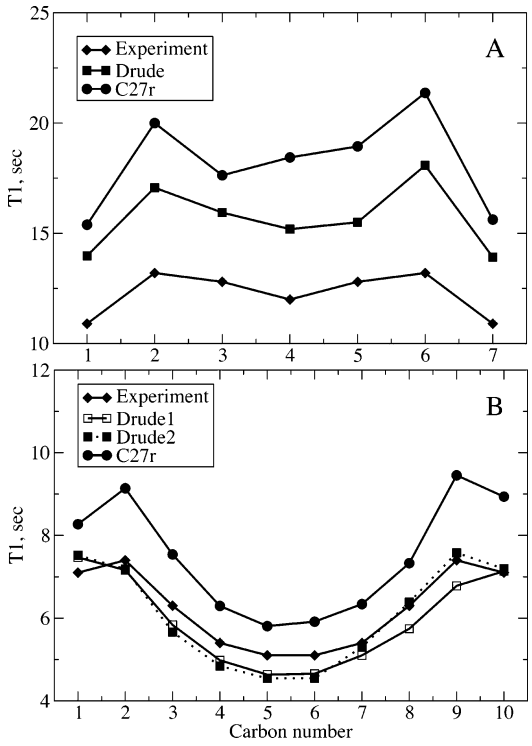

Figure 2. T_1 relaxation times for (A) heptane and (B) decane from experiment, the additive C27r, and the polarizable Drude model. Results from two separate simulations with the Drude model on decane are included in panel B.

3.5. Polarizability Scaling and Dielectric Constants. Proper treatment of the dielectric constant is an important quality of an empirical force field in order to accurately treat the extreme ranges of polarities that occur in biological systems. As mentioned in the Introduction, for the alkanes accurate treatment of the dielectric constants is particularly important for modeling solvation in hydrophobic environments given the relationship of the dielectric to the free energy of solvation based on the Born equation. Accordingly, this property was analyzed in detail. In addition, calculations of the dielectric constants allow for determination if scaling of the atomic polarizabilities to properly treat the condensed phase[39,75,104] is required for the alkanes as has been shown to be necessary for water[75,104] and DNA.[77]

Presented in Table 9 are the dielectric constants calculated for the neat alkane liquids. For the Drude model the overall

TABLE 9: Comparison of Experimental and Calculated Static Dielectric Constants of Neat Alkanes

	T, K	exptl ϵ[a]	C27r ϵ	Drude ϵ	Drude ϵ_∞
ethane	184.55	1.7595	1.0144 ± 0.0002	1.7068 ± 0.0053	1.6966 ± 0.0051
propane	231.08	1.7957	1.0153 ± 0.0001	1.7980 ± 0.0082	1.7684 ± 0.0078
propane[b]	231.08	1.7957		1.5493 ± 0.0051	1.5200 ± 0.0047
butane	272.65	1.8098	1.0155 ± 0.0001	1.8009 ± 0.0070	1.7742 ± 0.0066
isobutane	261.43	1.8176	1.0151 ± 0.0001	1.9046 ± 0.0093	1.8229 ± 0.0067
heptane	298.15	1.9113	1.0180 ± 0.0002	2.0210 ± 0.0070	1.9770 ± 0.0065
heptane	312.15	1.8904	1.0175 ± 0.0002	1.9760 ± 0.0087	1.9329 ± 0.0081
decane	298.15	1.9846	1.0196 ± 0.0002	2.1181 ± 0.0122	2.0655 ± 0.0115
decane	312.15	1.9668	1.0191 ± 0.0002	2.1276 ± 0.0094	2.0737 ± 0.0089

[a] Experimental values are from ref 66. [b] The atomic polarizabilities scaled by a factor of 0.724 were used in this simulation.

TABLE 10: Comparison of Experimental and Calculated Solvation Free Energies in the Aqueous Solution[a]

	ethane				butane		
	exptl	Drude	C27r		exptl	Drude	C27r
ΔG^{rep}		9.81	9.05	ΔG^{rep}		14.12	12.82
ΔG^{disp}		−7.76	−6.84	ΔG^{disp}		−12.34	−10.59
ΔG^{np}		2.06	2.21	ΔG^{np}		1.78	2.24
ΔG^{el}		−0.22	−0.05	ΔG^{el}		−0.31	−0.09
ΔG_{sol}	**1.77**	**1.84**	**2.17**	ΔG_{sol}	**2.15**	**1.46**	**2.15**
	propane				isobutane		
	exptl	Drude	C27r		exptl	Drude	C27r
ΔG^{rep}		12.18	10.79	ΔG^{rep}		14.55	12.29
ΔG^{disp}		−10.22	−8.75	ΔG^{disp}		−11.90	−10.35
ΔG^{np}		1.96	2.04	ΔG^{np}		2.65	1.94
ΔG^{el}		−0.33	−0.06	ΔG^{el}		−0.47	−0.08
ΔG_{sol}	**1.98**	**1.63**	**1.98**	ΔG_{sol}	**2.28**	**2.19**	**1.86**

[a] Energies in kcal/mol. $\Delta G^{np} = \Delta G^{rep} + \Delta G^{disp}$. Experimental data are from ref 14.

agreement with experiment is excellent, while the C27r values are all close to one due to the omission of explicit electronic polarizability in the model. The quality of the Drude results includes both the absolute values and the relative values between the different alkanes. These results were obtained using the atomic polarizabilities directly without scaling. When the fitted atomic polarizabilities were scaled by 0.724 for propane, as previously performed for water and a preliminary DNA polarizable model,[75,77] the resulting dielectric constant of the pure solvent is underestimated with respect to experiment (Table 9). Thus, in the case of the alkanes, it appears that scaling of the atomic polarizabilities from their gas phase values is not required to properly treat the condensed phase. This result suggests a model where the extent of scaling of the gas phase atomic polarizabilities is associated with the polarity or hydrogen bonding capacity of the compound. Current efforts are ongoing to address this issue via studies of a variety of polar liquids (A. D. MacKerell, Jr., B. Roux, and co-workers, work in progress). Thus, the developed polarizable model yields excellent agreement for the dielectric constant of the alkane pure solvents. This agreement along with the similar level of agreement of the Drude polarizable model for water suggest that the Drude model can accurately model the change in dielectric constant as a function of environment in biological systems.

3.6. Solvation Free Energy Calculation. A final test of the present aliphatic polarizable force field was the calculation of the free energies of the small alkanes in aqueous solution. Results, calculated using the approach developed by Deng and Roux,[97] are presented in Table 10, including results from experiment and C27r. In general, the agreement between the polarizable model and experiment is satisfactory; ethane and isobutane are in excellent agreement while the free energies of solvation of propane and butane are too favorable. In contrast, the C27r values are in good agreement for propane and butane, but in poorer agreement than the Drude model for ethane and isobutane.

The limited agreement of the polarizable free energies of aqueous solvation with experiment may, in part, be associated with convergence issues. The present results were obtained from 40 ps of sampling in each window following a 10 ps equilibration. Calculation of the free energies of solvation for the first and second 20 ps time periods from the 40 ps simulations for all systems yielded free energies that were less favorable for the second 20 ps periods. The values were 1.66/2.02, 1.52/1.81, 1.39/1.67, and 2.06/2.40 kcal/mol for ethane, propane, butane, and isobutane, respectively, where the values before and after the slash are for the first and second 20 ps periods, respectively. To check the impact of more sampling on the FEP results, longer simulations involving 50 ps of equilibration followed by 200 ps of sampling per window for propane were performed. The calculated solvation free energy from that calculation, 1.73 ± 0.13 kcal/mol (where the standard error was estimated using 50 ps block averages), is in slightly better agreement with the experimental value (see Table 10). These results indicate that longer simulations are required to obtain better convergence, although the result with the additional sampling is not significantly different from that presented in Table 10. The need for additional sampling to obtain a high level convergence is in agreement with a recent study in which over 1 ns of simulation time in each window was used to obtain results of high precision.[112,113] While such extensive sampling is, in principle, accessible using the polarizable model, it is beyond the scope of the present work. It should be emphasized that the solvation free energies were not explicitly used for the alkane parametrization but rather to confirm that developed parameters adequately describe condensed phase behavior not only in the nonpolar neat liquid alkanes but also in polar aqueous solution. Thus, the present aqueous free energies of solvation of the alkanes indicate the polarizable model to yield satisfactory agreement with experiment, though more extensive simulation studies are required to obtain better precision results.

3.7. Atomic Details of Nonbonding Interactions. Empirical force field based calculations are useful for understanding details of interactions between molecules at an atomic level of detail. Accordingly, it is of interest to know if the new polarizable force field has significant differences in the pair−pair correlation functions versus the additive, C27r model. Shown in Figure 3 are radial distribution functions from the propane pure solvent simulations (panels A and B) and from propane in aqueous solution (panels C and D). For the pure solvents it is evident that the $g(r)$ values are nearly identical for the additive and polarizable models. This similarity is not unexpected given the similarity of the LJ parameters for the two models and the minimal contribution of the electrostatic properties to the pure solvent properties. However, with propane in aqueous solution

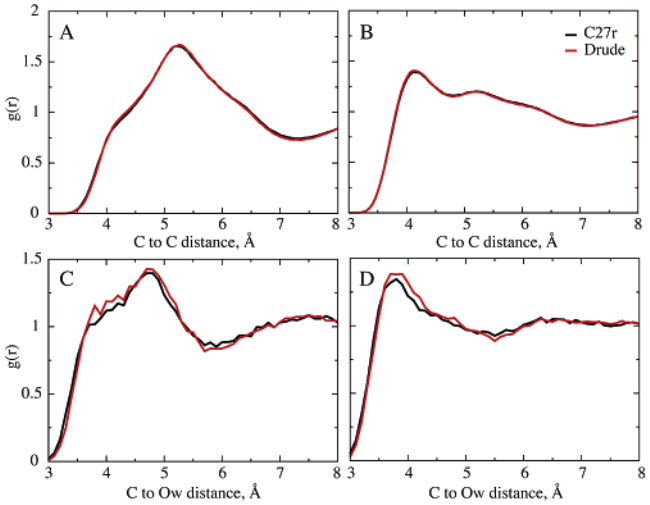

Figure 3. Radial distributions functions, $g(r)$, for the propane pure solvent (A) C1−C1 and (B) C2−C2 pairs and for propane in aqueous solution for the (C) C1−Ow and (D) C2−Ow pairs.

there are notable differences. For both the C1−Ow and C2−Ow $g(r)$ values the first peak is higher in the polarizable model. As the pure solvent $g(r)$ values are so similar this difference may be assumed to be dominated by the SWM4-NDP solvent model. However, the fact that there are differences indicates that the polarizable model does yield a somewhat different picture of the atomic details of the interactions of alkanes with the aqueous environment.

4. Conclusions

Presented is a polarizable force field for alkanes based on the use of a classical Drude oscillator for treatment of the electronic polarizability. Determination of the electrostatic parameters, q_i and α_i, was performed following a previously published protocol[77] based on B3LYP/aug-cc-pVDZ electrostatic potentials in the presence of perturbation ions. Fitting was based on the molecules ethane, propane, butane, pentane, and isobutane. To allow for transferability of the electrostatic parameters, consensus values were obtained for the CH_3, CH_2, and CH moieties. The availability of transferable electrostatic terms for the aliphatic moieties will facilitate the development of a broad force field for biological macromolecules, including the hydrophobic portions of lipids.

Explicit checks of the remainder of the parameters, including both internal and LJ terms, were performed. It was shown that the bond, angle, and Urey−Bradley terms could be transferred directly from the CHARMM27 force field, yielding satisfactory agreement with target data for the geometries and vibrational spectra. Such transfer appears to be due to the small impact of the electrostatic terms on the geometries and vibrations and is probably not appropriate with polar molecules. Consistent with this was the need to optimize the dihedral parameters to reproduce previously published QM data. LJ parameter optimization included reproduction of the relative interactions of He and Ne with the model compounds to reproduce QM data and of experimental condensed phase data for the neat alkanes. The combination of internal, LJ, and electrostatic parameters for the small alkanes yields reasonable agreement for the free energies of aqueous solvation of ethane, propane, butane, and isobutane, although further studies addressing the convergence of the obtained free energies are needed.

The parameters based on the lower alkanes were tested with respect to applicability to longer alkanes. Pure solvent simulations of heptane and decane yield good agreement with experiment for the molecular volume and heat of vaporizaiton. However, the self-diffusion constants are 5% to 11% smaller than experimental values. In contrast, the T_1 NMR relaxation times for decane are in good agreement with experiment, although they are overestimated for heptane, though to a lesser extent than observed with C27r. The discrepancy between the self-diffusion constants and the T_1 values is consistent with a previous suggestion[5] that limitations in the molecule shape may be responsible. These results indicate that the developed aliphatic parameters are transferable to larger alkanes, including those comprising lipids.

An important property of the resulting polarizable force field is the accurate treatment of the dielectric constant of the pure solvents. Additive force fields cannot reproduce the dielectric constant of approximately 2 for the neat alkanes due to the lack of explicit polarizability. Inclusion of polarizability via the classical Drude oscillator can accurately reproduce the dielectric constants, including the relative ordering among the alkanes. Notable is the lack of a need to scale the gas phase atomic polarizabilities to properly treat the condensed phase, as has been shown to be required for water and other polar solvents[39,75,77,104] (A. D. MacKerell, Jr., B. Roux, work in progress), suggesting that the polar character of the molecules, including the ability to hydrogen bond, may impact the need for scaling. Further studies will be required to clarify this point.

Acknowledgment. Financial support is acknowledged from the NIH (GM 51501) and we thank DOD ACS Major Shared Resource Computing and PSC Pittsburgh Supercomputing Center for their generous CPU allocations. The authors also appreciate helpful discussions with Drs. Benoit Roux, Jeff Klauda, Adam Moser, Yuqing Deng, and Guillaume Lamoureux.

Supporting Information Available: Experimental, C27r, and Drude alkane geometric parameters and vibrational frequencies; QM, C27r, and Drude barrier heights and plots for rotation around the C−C−C−C dihedral angle; corresponding C27r and Drude dihedral parameters; QM, C27r, and Drude minimum interaction energies and distances for complexes of alkane with helium and neon atoms; and parameters of the additive TIP3P and Drude polarizable SWM4-NDP water models. This material is available free of charge via the Internet at http://pubs.acs.org.

References and Notes

(1) Smith, J. C.; Karplus, M. *J. Am. Chem. Soc.* **1992**, *114*, 801.
(2) Zhang, Y. H.; Venable, R. M.; Pastor, R. W. *J. Phys. Chem.* **1996**, *100*, 2652.
(3) Yin, D.; MacKerell, A. D., Jr. *J. Comput. Chem.* **1998**, *19*, 334.
(4) Feller, S. E.; MacKerell, A. D., Jr. *J. Phys. Chem. B* **2000**, *104*, 7510.
(5) Klauda, J. B.; Brooks, B. R.; MacKerell, A. D.; Venable, R. M.; Pastor, R. W. *J. Phys. Chem. B* **2005**, *109*, 5300.
(6) Daura, X.; Mark, A. E.; van Gunsteren, W. F. *J. Comput. Chem.* **1998**, *19*, 535.
(7) Oostenbrink, C.; Villa, A.; Mark, A. E.; van Gunsteren, W. F. *J. Comput. Chem.* **2004**, *25*, 1656.
(8) Schuler, L. D.; Daura, X.; Van Gunsteren, W. F. *J. Comput. Chem.* **2001**, *22*, 1205.
(9) Schuler, L. D.; van Gunsteren, W. F. *Mol. Simul.* **2000**, *25*, 301.
(10) Kaminski, G.; Duffy, E. M.; Matsui, T.; Jorgensen, W. L. *J. Phys. Chem.* **1994**, *98*, 13077.
(11) Kaminski, G.; Jorgensen, W. L. *J. Phys. Chem.* **1996**, *100*, 18010.
(12) Jorgensen, W. L.; Maxwell, D. S.; Tirado-Rives, J. *J. Am. Chem. Soc.* **1996**, *118*, 11225.
(13) Miwa, Y.; Machida, K. *J. Am. Chem. Soc.* **1988**, *110*, 5183.
(14) Ben-Naim, A.; Marcus, Y. *J. Chem. Phys.* **1984**, *81*, 2016.
(15) Wallqvist, A.; Covell, D. G. *J. Phys. Chem.* **1995**, *99*, 13118.
(16) Mancera, R. L.; Buckingham, A. D. *J. Phys. Chem.* **1995**, *99*, 14632.
(17) Laidig, K. E.; Daggett, V. *J. Phys. Chem.* **1996**, *100*, 5616.

(18) Mundy, C. J.; Klein, M. L.; Siepmann, J. I. *J. Phys. Chem.* **1996**, *100*, 16779.
(19) Madan, B.; Sharp, K. *J. Phys. Chem. B* **1997**, *101*, 11237.
(20) Martin, M. G.; Siepmann, J. I. *J. Am. Chem. Soc.* **1997**, *119*, 8921.
(21) Chen, B.; Martin, M. G.; Siepmann, J. I. *J. Phys. Chem. B* **1998**, *102*, 2578.
(22) McGann, M. R.; Lacks, D. J. *J. Phys. Chem. B* **1999**, *103*, 2796.
(23) Gallicchio, E.; Kubo, M. M.; Levy, R. M. *J. Phys. Chem. B* **2000**, *104*, 6271.
(24) Chen, B.; Siepmann, J. I. *J. Phys. Chem. B* **1999**, *103*, 5370.
(25) Cui, Q. Z.; Smith, V. H. *J. Chem. Phys.* **2001**, *115*, 2228.
(26) Delhommelle, J.; Boutin, A.; Tavitian, B.; Mackie, A. D.; Fuchs, A. H. *Mol. Phys.* **1999**, *96*, 1517.
(27) Maple, J. R.; Hwang, M. J.; Stockfisch, T. P.; Hagler, A. T. *Isr. J. Chem.* **1994**, *34*, 195.
(28) Martin, M. G.; Siepmann, J. I. *J. Phys. Chem. B* **1999**, *103*, 4508.
(29) Nath, S. K.; De Pablo, J. J. *Mol. Phys.* **2000**, *98*, 231.
(30) Nath, S. K.; Escobedo, F. A.; de Pablo, J. J. *J. Chem. Phys.* **1998**, *108*, 9905.
(31) Nicolas, J. P.; Smit, B. *Mol. Phys.* **2002**, *100*, 2471.
(32) Rivera, J. L.; McCabe, C.; Cummings, P. T. *Phys. Rev. E* **2003**, *67*, 011603.
(33) Siepmann, J. I.; Martin, M. G.; Mundy, C. J.; Klein, M. L. *Mol. Phys.* **1997**, *90*, 687.
(34) Lee, S. H.; Lee, H.; Pak, H. *Bull. Korean Chem. Soc.* **1997**, *18*, 478.
(35) Lee, S. H.; Lee, H.; Pak, H. *Bull. Korean Chem. Soc.* **1997**, *18*, 501.
(36) Lee, S. H.; Lee, H.; Pak, H.; Rasaiah, J. C. *Bull. Korean Chem. Soc.* **1996**, *17*, 735.
(37) Sun, Y.; Spellmeyer, D.; Pearlman, D. A.; Kollman, P. *J. Am. Chem. Soc.* **1992**, *114*, 6798.
(38) Patel, S.; Brooks, C. L., III. *J. Comput. Chem.* **2004**, *25*, 1.
(39) Kaminski, G. A.; Stern, H. A.; Berne, B. J.; Friesner, R. A. *J. Phys. Chem. A* **2004**, *108*, 621.
(40) Zhang, Q.; Yang, Z. Z. *Chem. Phys. Lett.* **2005**, *403*, 242.
(41) Jorgensen, W. L.; Madura, J. D.; Swenson, C. J. *J. Am. Chem. Soc.* **1984**, *106*, 6638.
(42) Cornell, W. D.; Cieplak, P.; Bayly, C. I.; Gould, I. R.; Merz, K. M.; Ferguson, D. M.; Spellmeyer, D. C.; Fox, T.; Caldwell, J. W.; Kollman, P. A. *J. Am. Chem. Soc.* **1995**, *117*, 5179.
(43) Weiner, S. J.; Kollman, P. A.; Nguyen, D. T.; Case, D. A. *J. Comput. Chem.* **1986**, *7*, 230.
(44) Weiner, S. P.; Kollman, P. A.; Case, D. A.; Singh, U. C.; Ghio, C.; Alagona, G.; Profeta, S.; Weiner, P. *J. Am. Chem. Soc.* **1984**, *106*, 765.
(45) Allinger, N. L.; Yuh, Y. H.; Lii, J.-H. *J. Am. Chem. Soc.* **1989**, *111*, 8551.
(46) Lii, J.-H.; Allinger, N. L. *J. Am. Chem. Soc.* **1989**, *111*, 8566.
(47) Lii, J.-H.; Allinger, N. L. *J. Am. Chem. Soc.* **1989**, *111*, 8576.
(48) Allinger, N. L.; Chen, K. S.; Lii, J. H. *J. Comput. Chem.* **1996**, *17*, 642.
(49) Halgren, T. A. *J. Comput. Chem.* **1996**, *17*, 490.
(50) Halgren, T. A. *J. Comput. Chem.* **1996**, *17*, 553.
(51) Halgren, T. A.; Nachbar, R. B. *J. Comput. Chem.* **1996**, *17*, 587.
(52) Bordner, A. J.; Cavasotto, C. N.; Abagyan, R. A. *J. Phys. Chem. B* **2003**, *107*, 9601.
(53) Chang, J.; Sandler, S. I. *J. Chem. Phys.* **2004**, *121*, 7474.
(54) Derreumaux, P.; Dauchez, M.; Vergoten, G. *J. Mol. Struct.* **1993**, *295*, 203.
(55) Dillen, J. L. M. *J. Comput. Chem.* **1995**, *16*, 595.
(56) Dillen, J. L. M. *J. Comput. Chem.* **1995**, *16*, 610.
(57) Engelsen, S. B.; Fabricius, J.; Rasmussen, K. *Acta Chem. Scand.* **1994**, *48*, 553.
(58) Hwang, M. J.; Stockfisch, T. P.; Hagler, A. T. *J. Am. Chem. Soc.* **1994**, *116*, 2515.
(59) Maple, J. R.; Hwang, M. J.; Stockfisch, T. P.; Dinur, U.; Waldman, M.; Ewig, C. S.; Hagler, A. T. *J. Comput. Chem.* **1994**, *15*, 162.
(60) Nath, S. K.; Khare, R. *J. Chem. Phys.* **2001**, *115*, 10837.
(61) Palmo, K.; Mirkin, N. G.; Pietila, L. O.; Krimm, S. *Macromolecules* **1993**, *26*, 6831.
(62) Sun, H. *J. Phys. Chem. B* **1998**, *102*, 7338.
(63) Zhang, H. Z.; Ely, J. F. *Fluid Phase Equilib.* **2004**, *217*, 111.
(64) Foloppe, N.; MacKerell, A. D., Jr. *J. Comput. Chem.* **2000**, *21*, 86.
(65) Debolt, S. E.; Kollman, P. A. *J. Am. Chem. Soc.* **1995**, *117*, 5316.
(66) *CRC Handbook Chemistry and Physics*, 84th ed.; Lide, D. R., Ed.; CRC Press: Boca Raton, FL, 2003.
(67) Leach, A. R. *Molecular Modelling*: *Principles and Applications*; Longman: Harlow, UK, 1996.
(68) Drude, P.; Mann, C. R.; Millikan, R. A. *The theory of optics*; Longmans, Green, and Co.: New York, 1902.
(69) Hoye, J. S.; Stell, G. *J. Chem. Phys.* **1980**, *73*, 461.
(70) Pratt, L. R. *Mol. Phys.* **1980**, *40*, 347.
(71) Cao, J. S.; Berne, B. J. *J. Chem. Phys.* **1993**, *99*, 6998.
(72) Stuart, S. J.; Berne, B. J. *J. Phys. Chem.* **1996**, *100*, 11934.
(73) Lado, F. *J. Chem. Phys.* **1997**, *106*, 4707.
(74) Lamoureux, G.; Roux, B. *J. Chem. Phys.* **2003**, *119*, 3025.
(75) Lamoureux, G.; MacKerell, A. D., Jr.; Roux, B. *J. Chem. Phys.* **2003**, *119*, 5185.
(76) Noskov, S. Y.; Lamoureux, G.; Roux, B. *J. Phys. Chem. B* **2005**, *109*, 6705.
(77) Anisimov, V. M.; Lamoureux, G.; Vorobyov, I. V.; Huang, N.; Roux, B.; MacKerell, A. D., Jr. *J. Chem. Theory Comput.* **2005**, *1*, 153.
(78) Frisch, M. J.; Trucks, G. W.; Schlegel, H. B.; Scuseria, G. E.; Robb, M. A.; Cheeseman, J. R.; Zakrzewski, V. G.; Montgomery, J. A., Jr.; Stratmann, R. E.; Burant, J. C.; Dapprich, S.; Millam, J. M.; Daniels, A. D.; Kudin, K. N.; Strain, M. C.; Farkas, O.; Tomasi, J.; Barone, V.; Cossi, M.; Cammi, R.; Mennucci, B.; Pomelli, C.; Adamo, C.; Clifford, S.; Ochterski, J.; Petersson, G. A.; Ayala, P. Y.; Cui, Q.; Morokuma, K.; Malick, D. K.; Rabuck, A. D.; Raghavachari, K.; Foresman, J. B.; Cioslowski, J.; Ortiz, J. V.; Baboul, A. G.; Stefanov, B. B.; Liu, G.; Liashenko, A.; Piskorz, P.; Komaromi, I.; Gomperts, R.; Martin, R. L.; Fox, D. J.; Keith, T.; Al-Laham, M. A.; Peng, C. Y.; Nanayakkara, A.; Gonzalez, C.; Challacombe, M.; Gill, P. M. W.; Johnson, B.; Chen, W.; Wong, M. W.; Andres, J. L.; Gonzalez, C.; Head-Gordon, M.; Replogle, E. S.; Pople, J. A. *Gaussian 98*; Gaussian, Inc.: Pittsburgh, PA, 1998.
(79) Frisch, M. J.; Trucks, G. W.; Robb, M. A.; Scuseria, G. E.; Schlegel, H. B.; Cheeseman, J. R.; Montgomery, J. A., Jr.; Vreven, T.; Kudin, K. N.; Burant, J. C.; Millam, J. M.; Iyengar, S. S.; Tomasi, J.; Barone, V.; Mennucci, B.; Cossi, M.; Scalmani, G.; Rega, N.; Petersson, G. A.; Nakatsuji, H.; Hada, M.; Ehara, M.; Toyota, K.; Fukuda, R.; Hasegawa, J.; Ishida, M.; Nakajima, T.; Honda, Y.; Kitao, O.; Nakai, H.; Klene, M.; Li, X.; Knox, J. E.; Hratchian, H. P.; Cross, J. B.; Bakken, V.; Adamo, C.; Jaramillo, J.; Gomperts, R.; Stratmann, R. E.; Yazyev, O.; Austin, A. J.; Cammi, R.; Pomelli, C.; Ochterski, J. W.; Ayala, P. Y.; Morokuma, K.; Voth, G. A.; Salvador, P.; Dannenberg, J. J.; Zakrzewski, V. G.; Dapprich, S.; Daniels, A. D.; Strain, M. C.; Farkas, O.; Malick, D. K.; Rabuck, A. D.; Raghavachari, K.; Foresman, J. B.; Ortiz, J. V.; Cui, Q.; Baboul, A. G.; Clifford, S.; Cioslowski, J.; Stefanov, B. B.; Liu, G.; Liashenko, A.; Piskorz, P.; Komaromi, I.; Martin, R. L.; Fox, D. J.; Keith, T.; Al-Laham, M. A.; Peng, C. Y.; Nanayakkara, A.; Challacombe, M.; Gill, P. M. W.; Johnson, B.; Chen, W.; Wong, M. W.; Gonzalez, C.; Pople, J. A. *Gaussian 03*, Revision C.02; Gaussian, Inc.: Wallingford, CT, 2004.
(80) Becke, A. D. *Phys. Rev. A* **1988**, *38*, 3098.
(81) Becke, A. D. *J. Chem. Phys.* **1993**, *98*, 5648.
(82) Lee, C.; Yang, W.; Parr, R. G. *Phys. Rev. B* **1988**, *37*, 785.
(83) Dunning, T. H. *J. Chem. Phys.* **1989**, *90*, 1007.
(84) Brooks, B. R.; Bruccoleri, R. E.; Olafson, B. D.; States, D. J.; Swaminathan, S.; Karplus, M. *J. Comput. Chem.* **1983**, *4*, 187.
(85) MacKerell, A. D., Jr.; Brooks, B.; Brooks, C. L., III; Nilsson, L.; Roux, B.; Won, Y.; Karplus, M. CHARMM: The Energy Function and Its Paramerization with an Overview of the Program. In *Encyclopedia of Computational Chemistry*; Schleyer, P. v. R., Allinger, N. L., Clark, T., Gasteiger, J., Kollman, P. A., Schaefer, H. F., III, Schreiner, P. R., Eds.; John Wiley & Sons: Chichester, UK, 1998; Vol. 1; p 271.
(86) Thole, B. T. *Chem. Phys.* **1981**, *59*, 341.
(87) Ryckaert, J. P.; Ciccotti, G.; Berendsen, H. J. C. *J. Comput. Phys.* **1977**, *23*, 327.
(88) Darden, T. A.; York, D.; Pedersen, L. G. *J. Chem. Phys.* **1993**, *98*, 10089.
(89) Steinbach, P. J.; Brooks, B. R. *J. Comput. Chem.* **1994**, *15*, 667.
(90) Lague, P.; Pastor, R. W.; Brooks, B. R. *J. Phys. Chem. B* **2004**, *108*, 363.
(91) Allen, M. P.; Tildesley, D. J. *Computer Simulation of Liquids*; Clarendon Press: Oxford, UK, 1987.
(92) Ottiger, M.; Bax, A. *J. Am. Chem. Soc.* **1998**, *120*, 12334.
(93) Bonin, K. D.; Kresin, V. V. *Electric-dipole polarizabilities of atoms, molecules, and clusters*; World Scientific: River Edge, NJ, 1997.
(94) Neumann, M.; Steinhauser, O. *Chem. Phys. Lett.* **1984**, *106*, 563.
(95) Simonson, T. Free Energy Calculations. In *Computational Biochemistry and Biophysics*; Becker, O. M., MacKerell, A. D., Jr., Roux, B., Watanabe, M., Eds.; Marcel Dekker: New York, 2001; p 169.
(96) Kollman, P. *Chem. Rev.* **1993**, *93*, 2395.
(97) Deng, Y.; Roux, B. *J. Phys. Chem. B* **2004**, *108*, 16567.
(98) Weeks, J. D.; Chandler, D.; Andersen, H. C. *J. Chem. Phys.* **1971**, *54*, 5237.
(99) Kumar, S.; Bouzida, D.; Swendsen, R. H.; Kollman, P. A.; Rosenberg, J. M. *J. Comput. Chem.* **1992**, *13*, 1011.
(100) Lamoureux, G.; Harder, E.; Vorobyov, I.; Deng, Y.; Roux, B.; MacKerell, A. D., Jr. Manuscript in preparation.
(101) Jorgensen, W. L.; Chandrasekhar, J.; Madura, J. D.; Impey, R. W.; Klein, M. L. *J. Chem. Phys.* **1983**, *79*, 926.
(102) Anisimov, V. M.; Vorobyov, I. V.; Lamoureux, G.; Noskov, S.; Roux, B.; MacKerell, A. D., Jr. *Biophys. J.* **2004**, *86*, 415a.
(103) Morita, A.; Kato, S. *J. Chem. Phys.* **1999**, *110*, 11987.
(104) Giese, T. J.; York, D. M. *J. Chem. Phys.* **2004**, *120*, 9903.

(105) in het Panhuis, M. P.; Popelier, P. L. A.; Munn, R. W.; Angyan, J. G. *J. Chem. Phys.* **2001**, *114*, 7951.
(106) Tu, Y. Q.; Laaksonen, A. *Chem. Phys. Lett.* **2000**, *329*, 283.
(107) Miller, K. J. *J. Am. Chem. Soc.* **1990**, *112*, 8533.
(108) MacKerell, A. D., Jr.; Bashford, D.; Bellott, M.; Dunbrack, R. L., Jr.; Evanseck, J.; Field, M. J.; Fischer, S.; Gao, J.; Guo, H.; Ha, S.; Joseph, D.; Kuchnir, L.; Kuczera, K.; Lau, F. T. K.; Mattos, C.; Michnick, S.; Ngo, T.; Nguyen, D. T.; Prodhom, B.; Reiher, W. E., III; Roux, B.; Schlenkrich, M.; Smith, J.; Stote, R.; Straub, J.; Watanabe, M.; Wiorkiewicz-Kuczera, J.; Yin, D.; Karplus, M. *J. Phys. Chem. B* **1998**, *102*, 3586.
(109) Chalasinski, G.; Szczesniak, M. M. *Chem. Rev.* **1994**, *94*, 1723.
(110) Jeziorski, B.; Moszynski, R.; Szalewicz, K. *Chem. Rev.* **1994**, *94*, 1887.
(111) Yin, D.; MacKerell, A. D., Jr. *J. Phys. Chem.* **1996**, *100*, 2588.
(112) Shirts, M. R.; Pitera, J. W.; Swope, W. C.; Pande, V. S. *J. Chem. Phys.* **2003**, *119*, 5740.
(113) Shirts, M. R.; Pande, V. S. *J. Chem. Phys.* **2005**, *122*.
(114) Smith, B. D.; Srivastava, R. *Thermodynamic data for pure compounds, Part A. Hydrocarbonds and ketones*; Elsevier: New York, 1986.
(115) *NIST Chemistry WebBook*; NIST Standard Reference Database No. 69; Linstrom, P. J., Mallard, W. G., Eds.; National Institute of Standards and Technology: Gaithersburg, MD 20899 (http://webbook.nist.gov), 2005.
(116) Ertl, H.; Dullien, F. A. L. *AIChE J.* **1973**, *19*, 1215.